

Characterization of Sepaku Clay Shale with Slaking Test, X-Ray Diffraction and Scanning Electron Microscopy: Potential Stabilization Using *Bacillus Subtilis*

Yuswal Subhy¹, Achmad Bakri Muhiddin², Ardy Arsyad²

¹Doctoral Student in Civil Engineering Program, Hasanuddin University, Makassar, Indonesia

²Lecturer at the Department of Civil Engineering, Hasanuddin University, Makassar, Indonesia

*Correspondence: yuswalsubhy1971@gmail.com

SUBMITTED 2 November 2025 REVISED 27 December 2025 ACCEPTED 28 December 2025

ABSTRACT Clay shale in the Sepaku region exhibits geotechnical vulnerability (slaking, cohesion loss, saturation expansion) that threatens slope stability and road foundations. Conventional stabilization methods (cement/lime) can cause negative environmental impact; therefore, alternatives with low environmental impact such as microbially induced carbonate precipitation (MICP) are sought for. MICP has the potential to improve the mechanical properties of clay shale. MICP utilizes microbial activity (urease enzyme or alternative pathways) to trigger CaCO_3 precipitation that binds soil particles and fills pores. In order to optimize the stabilization effects of MICP on Sepaku clay shale, it is first necessary to characterize the clay shale properties. Slaking test, X-Ray diffraction and scanning electron microscopy were conducted on clay shale samples obtained from Sepaku region. The SPT tests from two boreholes show NSPT values of above 60 for the shale, which is expected for unweathered shale. The disturbed samples were then subjected to slaking tests, which the results categorize the shale to be low durability after one cycle of wetting and drying, and very low durability after two cycles of wetting and drying. The unconfined compressive strength was found to be 2.53 MPa, categorizing the Sepaku clay as weak rock. The XRD and SEM results of Sepaku clay revealed consistent values and characteristics as other clay shales. This research serves as preliminary investigation to optimize the stabilization of Sepaku clay shale using MICP method, in particular *Bacillus Subtilis* bacteria.

KEYWORDS Clay Shale; XRD; SEM; MICP; *Bacillus-Subtilis*

1 INTRODUCTION

A number of areas in the East Kalimantan, particularly Ibu Kota Nusantara (IKN), Indonesia's new capital city, consist of clay shale. Clay shale (mudrock) is a cohesive lithology commonly found in various sedimentary basins and often exhibits mechanical behavior that is sensitive to changes in water content: slaking (weathering/cracking when wet), decreased cohesion when saturated, and expansion and contraction that can damage surface structures or foundations. It is important to understand degradation when exposed to the environment, which can change it from hard rock to soft clay, as well as its impact on slope stability and infrastructure (Johan et al., 2023; Nazir et al., 2024; Sagitaningrum et al., 2023). The sensitivity of clay shale to water poses major challenges that must be carefully addressed. Head of the IKN Authority, Basuki Hadimuljono, explained that the clay shale soil found in the IKN requires special treatment to make it stronger and more stable to support the various infrastructure projects that will be built in the region.

In the Sepaku area (IKN/Pamaluan Formation region), where the study area is, the presence of this weathered clay shale layer is of particular concern for infrastructure planning due to the potential for slope failure and reduced soil bearing capacity if not properly addressed. Figure 1 and 2 shows the study location, Jl. Negara, Sukaraja, Sepaku, Penajam Paser Utara, East Kalimantan, where boring test and clay shale sampling were taken from. Regional geological studies and local technical reports

recommend the need for stabilization strategies that consider the mineralogical characteristics and microstructure of the shale.

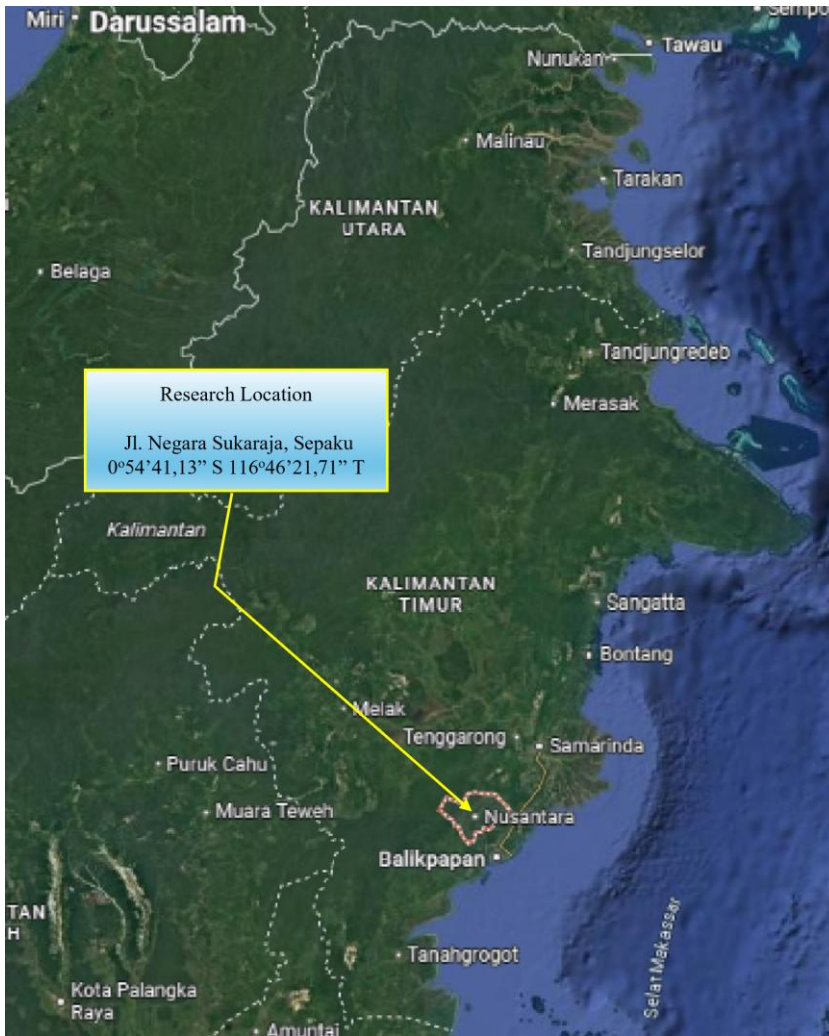


Figure 1. Map of East Kalimantan Province

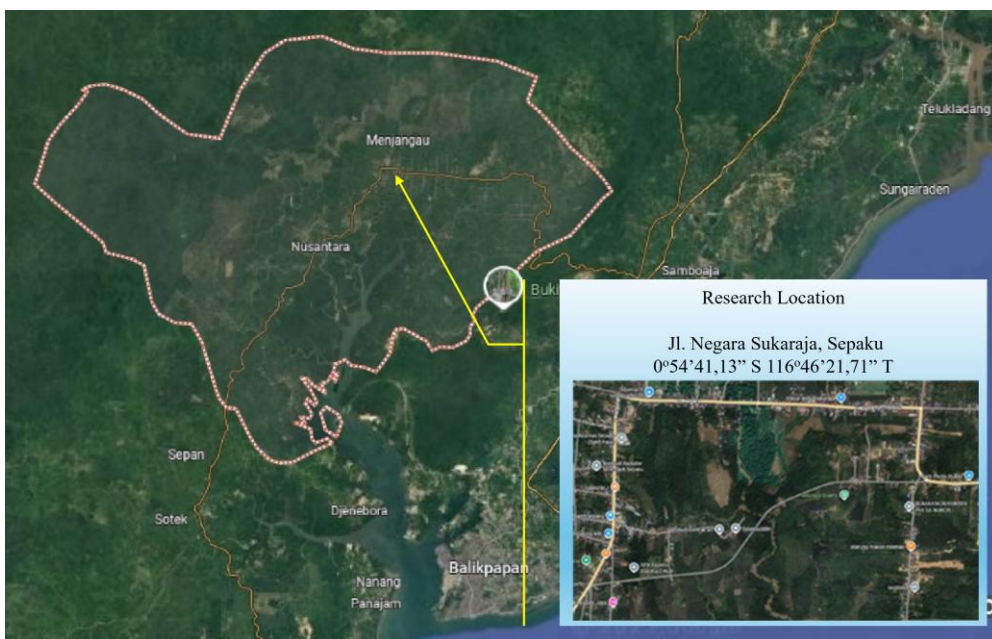


Figure 2. Map of Sepaku Subdistrict

Improvements in the mechanical properties of traditional soils/rocks generally use inorganic materials such as cement or lime. However, this approach often results in a large carbon footprint and environmental compatibility issues. In the past two decades, microbially induced carbonate precipitation (MICP) has emerged as an alternative biotechnical technique that can form intergranular calcite (CaCO_3) precipitation, thereby improving cohesion, reducing permeability, and increasing resistance to erosion or slaking with potentially lower environmental footprints when properly managed. A recent comprehensive review discusses the principles, control parameters, and engineering applications of MICP for soil improvement (Fu et al., 2023).

Recent literature suggests that in addition to ureolytic bacteria which is usually used for MICP (e.g. *Sporosarcina pasteurii*), *Bacillus subtilis*, both naturally and through genetic engineering (Hoffman et al., 2021), can also improve CaCO_3 biomineralization. Experimental research and genetic engineering studies on *Bacillus subtilis* demonstrate the ability of certain strains to facilitate carbonate precipitation, making them attractive candidates for clay shale stabilization that requires robust and easily cultured organisms. Many MICP studies, however, focus on sand and coarse-grained soils (Baek et al., 2024; Fronczyk et al., 2023; Ghasemi and Montoya, 2022; Gunyol et al., 2024; Harran et al., 2022; Konstantinou et al., 2021; Lin et al., 2023; Clarà Saracho et al., 2025; Wang et al., 2023; Sun et al., 2022; Xiao et al., 2025). Applications in fine/clay soils and clay shales remain challenging due to low permeability, ion adsorption on clay mineral surfaces, and natural laminated structures that affect reagent transport and precipitation locations.

In order to investigate the appropriateness of MICP to stabilize clay shale, it is first necessary to properly characterize the clay shale. The Sepaku clay shale obtained for this study was subjected to slaking tests and investigated under universal testing machine, X-Ray diffraction tests and scanning electron microscopy. This research serves as preliminary investigation in improving the standards for the use of clay shale material in the construction service industry in the Sepaku area, which has been chosen as the new capital city.

2 THEORETICAL BASIS

2.1 Characteristics of Clay Shale

The composition of clay shale generally consists of clay minerals (smectite/montmorillonite, illite, kaolinite) along with non-clay minerals (quartz, feldspar, calcite, iron oxide). The proportion and type of clay minerals greatly influence plasticity, water retention capacity, swelling/shrinking ability, and collapse mechanics; for example, a high smectite fraction is associated with high expansivity. Mineralogical changes due to weathering also alter the mechanical response of these rocks. General characteristics of clay shale are summarized in table 1.

Table 1. General characteristics of clay shale (from geological engineering literature)

Characteristics	Description
Composition	Dominated by clay minerals such as Illite, Kaolinite and Montmorillonite
Structure	Fine lamination (layered), often showing parallel fractures
Mechanical Behavior	Low strength, highly affected by moisture
Durability	Low resistance to wet-dry cycles (easily weathered)
Weathering Effects	Very susceptible to changes in properties due to chemical and physical weathering
Usability	Requires stabilization when used as fill material or foundation

Clay shale (weathered mudrock/claystone) in the Sepaku area (Pamaluan Formation and IKN region) also has potential geotechnical problems: slaking (rapid weathering when moisture content changes rapidly), loss of cohesion under saturated conditions, expansion/contraction, and strength reduction that affects slope and foundation stability. Regional geological studies and technical proceedings indicate the dominance of mudrock/claystone layers in the Pamaluan formation, which is relevant for engineering planning in Sepaku. (Sidharta, 2022).

To better understand clay shale characteristics, multi-analytical analysis, particularly XRD (X-Ray Diffraction), XRF (X-Ray Fluorescence), and SEM-EDS (Scanning Electron Microscope - Energy Dispersive X-ray Spectroscopy) are standard approaches for understanding mineral structure and mechanisms after stabilization treatment. XRD can be used to identify the mineral composition of clay (e.g., kaolinite, illite, smectite), while SEM-EDS is used to analyze surface morphology and elemental composition. This is important for identifying the swelling potential and reactivity of clay minerals (Jia et al., 2023; Ardebili et al., 2025). Studies characterizing modern shale confirm the importance of integrating XRD-XRF-SEM results for interpreting changes in pore and mineral matrix properties (Liu et al., 2024). Figure 3 to 10 shows some XRD and SEM results available in the literature.

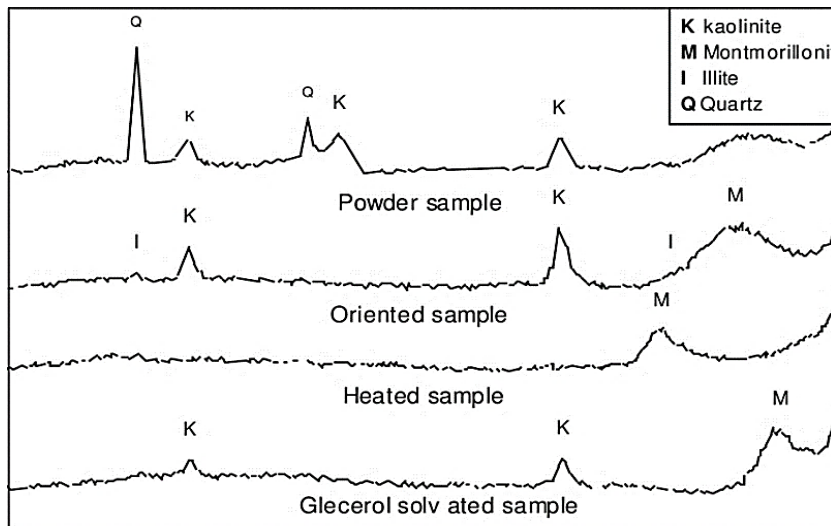


Figure 3. XRD pattern of shale/clay samples (Othman et al., 2003). *Description: XRD clay shale pattern, showing main diffraction peaks such as quartz, with clay mineral signals*

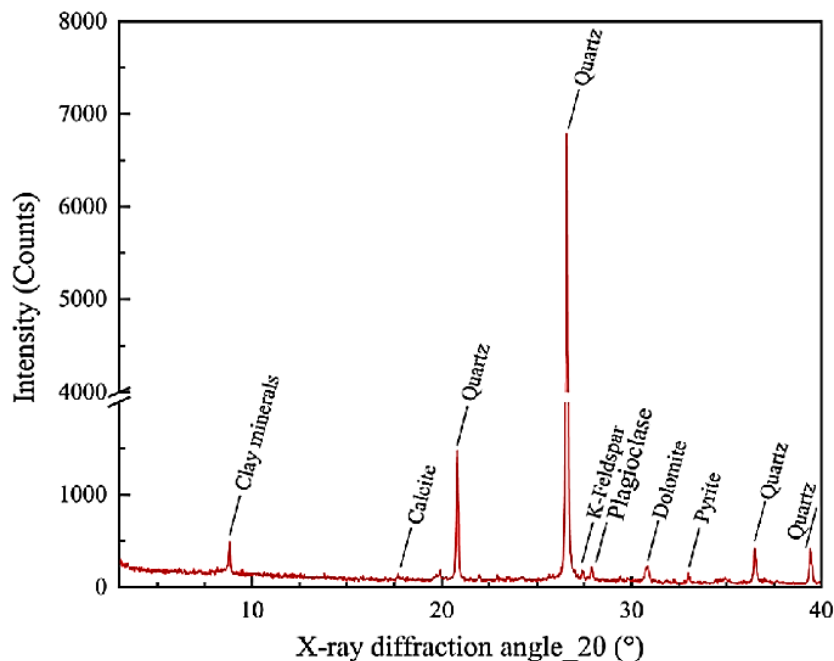


Figure 4. XRD pattern results from clay shale (Guo et al., 2023)

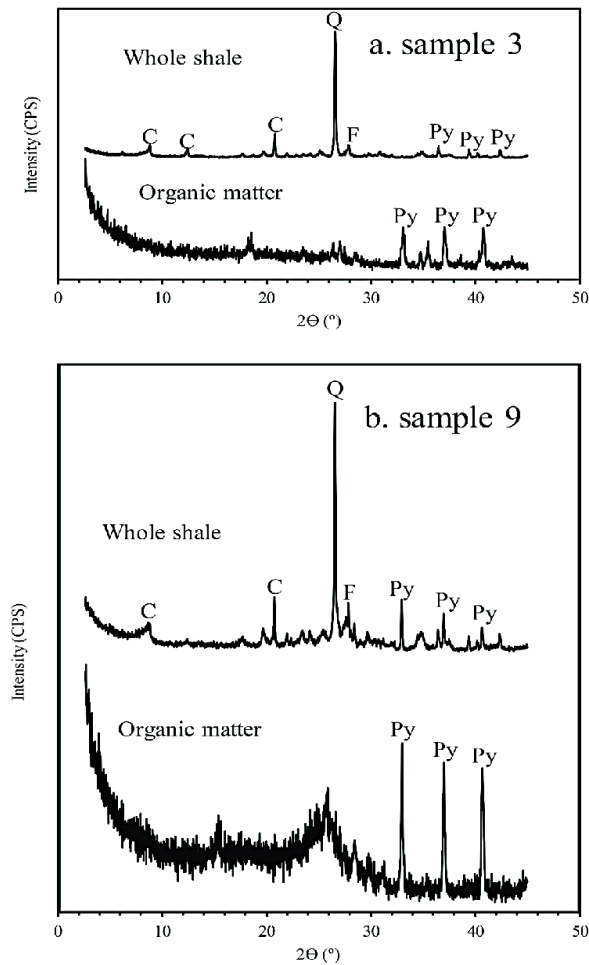


Figure 5. XRD patterns of intact shale and organic matter in sample 3 and sample 9. (C = Clay minerals. Q = Quartz. Py = Pyrite. F = Feldspar) (Han et al., 2019) *Description: XRD of whole shale and organic matter, identification of quartz, pyrite, clay minerals, feldspar.*

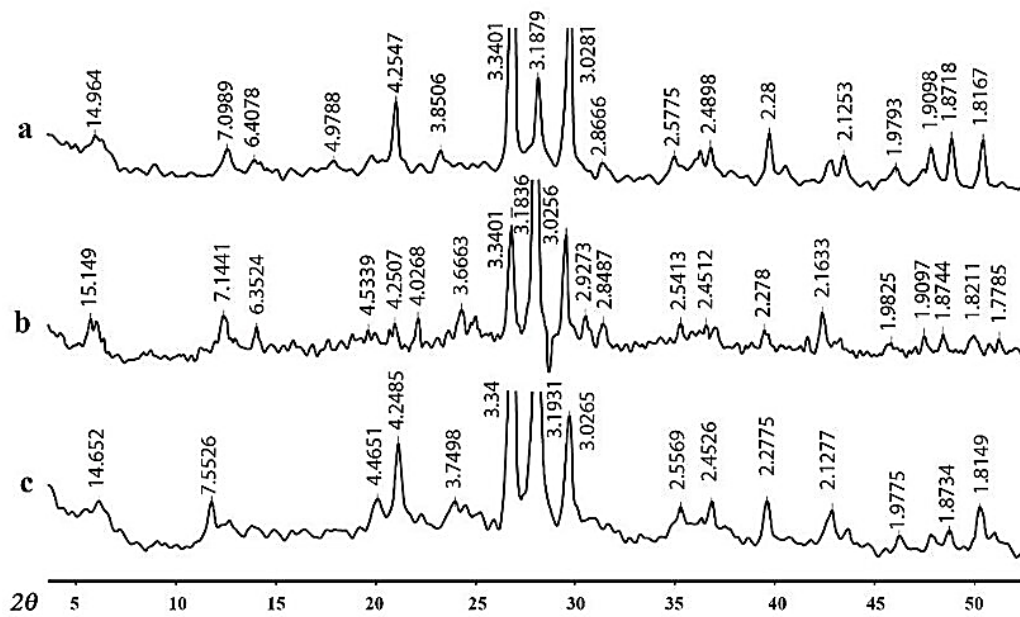


Figure 6. X-ray diffraction patterns of clay rocks: a-clay shale, b-argillite, c-clay (Shapakidze et al., 2023) *Description: Comparison of XRD patterns of shale, argillite, and clay; showing the characteristic peaks of each type of material.*

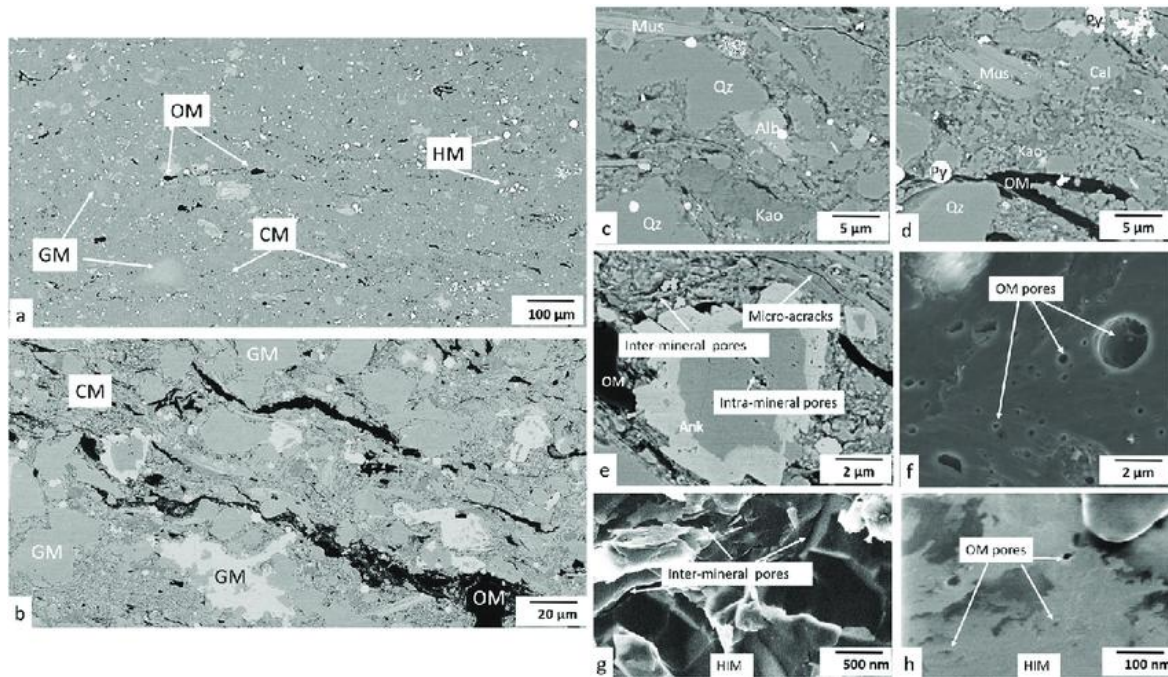


Figure 7. SEM (Scanning Electron Microscopy) test results of clay shale / shale with similar microstructures - showing pores, microcracks, clay mineral orientation, and organic matter. (Ma et al., 2021) *Description: SEM images of the Bowland formation. (a) General overview of the microstructure of the sample; (b) general overview of the microstructure of the sample at higher resolution; identification of (c) granular minerals and clay minerals; (d) heavy minerals and organic matter particles; (e) mineral pores and microcracks; (f) organic matter pores; (g) intermineral pores (taken with HIM); (h) organic matter pores (taken with HIM). GM - granular minerals, CM - clay minerals, OM - organic matter, HM - heavy minerals. Qz - quartz, Alb - albite, Cal - calcite, Ank - ankerite, Py - pyrite, Mus - muscovite, Kao - kaolinite. HIM - Helion ion microscopy.*

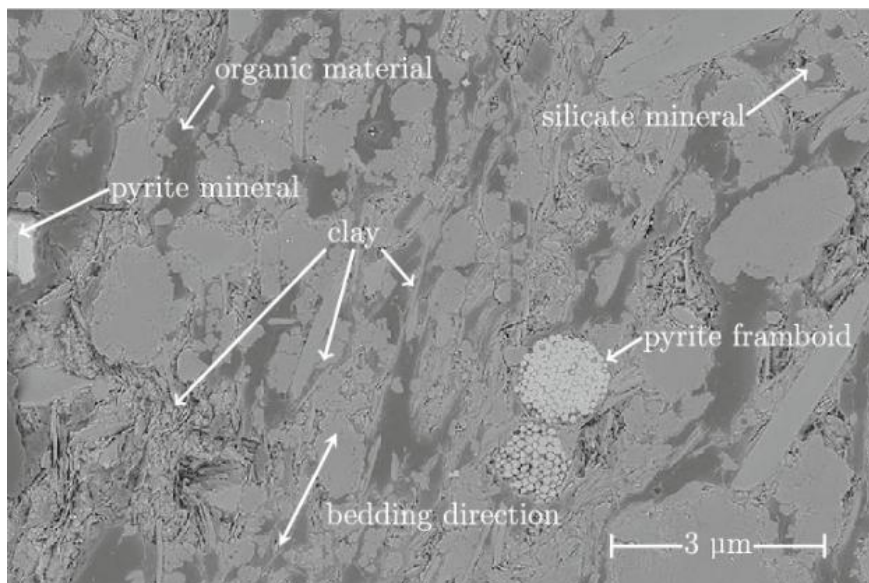


Figure 8. SEM test results of polished shale sample surfaces (Bennett et al., 2015). *Description: Polished shale surface, displaying microcracks and a rough surface as a result of clay particle fragments.*

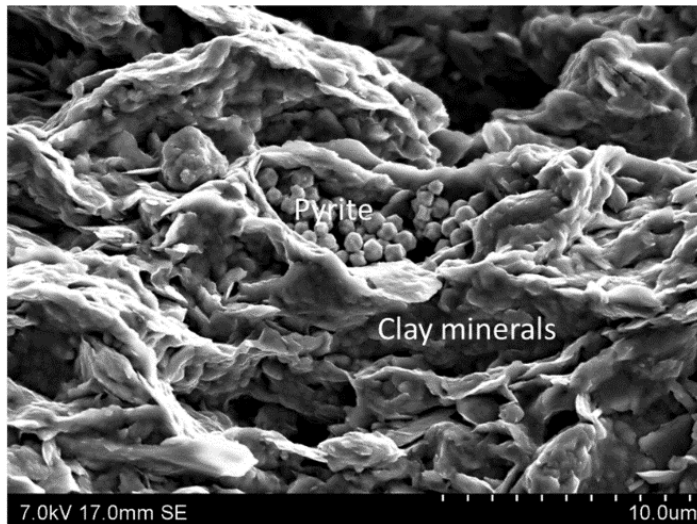


Figure 9. SEM test results from typical northern marine shale samples (Bhuiyan et al., 2020). *Description: Image of North Sea shale, showing the relationship between clay particles, small fractures, and intermineral pores*

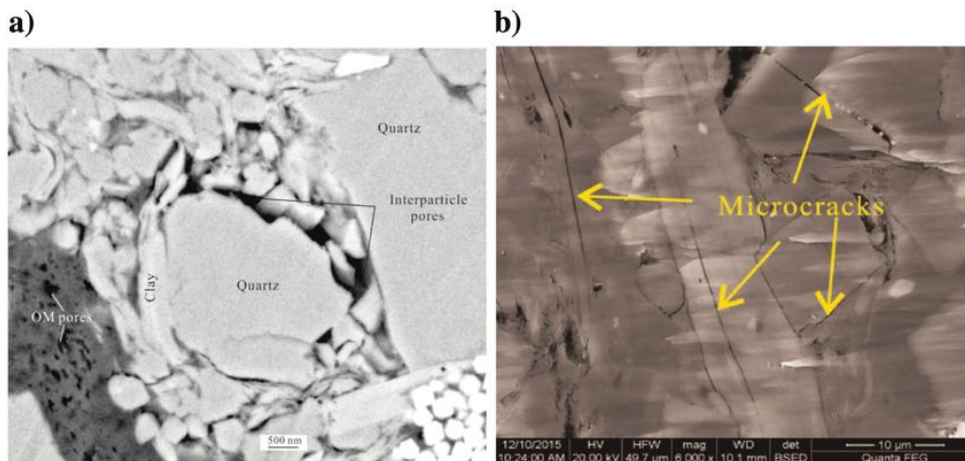


Figure 10. SEM microstructure test results of Longmaxi (Qi et al., 2021) *Description: Detailed image of intra-particle and inter-particle pores in organic-rich shale, showing fine voids within organic particles and between clay minerals and quartz.*

Given the properties of clay shale determined by mineralogy and microstructure, stabilization efforts using MICP should use approaches that modify the microstructure (e.g., inter-grain bonding) and be verified by mineralogical/chemical/microscopic characterization techniques (XRD, XRF, SEM/EDS).

2.2 Principles of Soil Bio-stabilization and Microbially Induced Carbonate Precipitation

Microbially Induced Carbonate Precipitation (MICP) is a biomineralization process in which ureolytic bacteria (urease) catalyze the hydrolysis of urea $(\text{NH}_2)_2\text{CO}$ into ammonia (NH_3) and carbon dioxide (CO_2) . The local increase in pH due to NH_3 produces carbonate ions (CO_3^{2-}) which react with calcium ions (Ca^{2+}) to form CaCO_3 precipitation (calcite/vaterite/aragonite). The reaction is shown in equations 1 to 3.



This precipitation fills pores and binds soil particles, thereby increasing cohesion and compressive strength and reducing permeability.

Critical parameters controlling MICP efficiency includes urease enzyme activity, availability of C/N sources (urea), Ca^{2+} concentration, pH, temperature, media permeability and injection/dosing scheme (Omorieg et al., 2025). Reviews and recent experimental studies conclude that MICP can be applied to improve surface strength, reduce erosion, and improve the rheological properties of fine soils when conditions and protocols are well controlled (Payan et al., 2024). In addition to ureolysis, other pathways (denitrification, photosynthesis, sulfate reduction, non-ureolytic pathways) can also produce carbonate; the selection of mechanisms must be tailored to the stabilization objectives and environmental conditions (Liu et al., 2024).

2.3 *Bacillus Subtilis* as a Biostabilization Agent – Evidence and Characteristics

Sporosarcina pasteurii is widely known as the standard ureolytic bacterium in many MICP studies, however, recent literature shows that *Bacillus subtilis* also has potential in biocementation applications. *Bacillus Subtilis* is a gram-positive bacterium capable of producing the urease enzyme, which plays a role in the process of microbially induced calcite precipitation (MICP). Ivanov & Stabnikov (2016), and Chu and Ivanov (2012) have shown that *Bacillus Sp* can be used to increase soil strength and reduce permeability through calcite precipitation between soil pores.

Several experimental studies and new isolates report that certain strains of *Bacillus subtilis* are capable (directly or through community/enzyme contributions) of facilitating CaCO_3 formation and improving surface/particle stability on various substrates (sand, laterite, construction materials). Research on environmentally resistant isolates demonstrates the application of *Bacillus subtilis* in arid regions (dust control) and confirmed the mineralization via SEM/XRD. However, urease characteristics and precise mechanisms may vary between strains, necessitating strain/isolate verification (Zakavi et al., 2024).

2.4 The Role of Characterization Techniques: XRD, XRF, SEM/EDS

To prove that *Bacillus subtilis* treatment produces CaCO_3 precipitation and changes the properties of clay shale, multi-technique evidence is needed:

- XRD (X-ray Diffraction): identification of the crystalline phase of CaCO_3 (calcite: peak $2\theta \sim 29.4^\circ$ on plane (104)) and quantification of phase changes (via Rietveld) to estimate the fraction of new carbonate. Routine MICP studies utilize XRD as evidence of the crystalline phase (Said et al., 2025).
- XRF (X-ray Fluorescence): quantification of Ca (CaO) element in crease and elemental ratio changes (Ca/Si, Ca/Al) that support the amount of Ca bound by carbonate. XRF provides an overview of bulk composition changes (Etim et al., 2025).
- SEM + EDS: visualization of precipitation morphology (crystal shape, pore filling, intergranular bridges) and elemental mapping to confirm CaCO_3 distribution at the micro scale. SEM/EDS also captures changes in clay surface structure and precipitation-particle interactions (Said et al., 2025).

The combination of all three (convergent evidence) is considered the best practice in literature for linking the formation of new minerals with changes in mechanical properties.

2.5 Results of Previous Studies and Relevance to Clay Shale

- According to Ivanov and Chu (2008), *Bacillus subtilis* has biomineralization capabilities, namely the precipitation of minerals (especially CaCO_3) in soil or rock pores, making it an efficient biological agent in soil stabilization or the improvement of soft rock structures such as clay shale or siltstone.
- Recent experiments (2024–2025) show that MICP can increase unconfined compressive strength (UCS), reduce permeability, and improve resistance to wetting drying cycles in

cohesive soils when parameters are optimized. However, many studies focus on loose soils (sand, laterite) rather than weathered clay shale with a laminated structure (Etim et al., 2025).

- Clay shale (weathered rock) has different permeability and physical structures (lamination, natural aggregation) so that reagent distribution and precipitation locations tend to be heterogeneous; the literature identifies the need for specific research on clay shale, including optimization of injection methods, pre-conditioning, and multi-instrument verification. The Sepaku geological study also highlights the vulnerability of mudrock to wet/dry conditions, making stabilization necessary and bio-stabilization an environmentally friendly stabilization method (Sidharta, 2022).
- As aforementioned, urease activity (depending on strain), is dependent on cell density, urea and Ca^{2+} concentrations, application method (mixing vs. injection/percolation), in-situ permeability, pH & temperature. However, for application in clay, clay surface chemical interactions also play a role. Ca^{2+} ions can be adsorbed to the clay surface, suppressing precipitation. Hence, for clay shale, special considerations are needed, such as low-rate injection, pre-drilling microchannels, or a combination of local mixing to ensure distribution (Lai et al., 2024).

2.6 Summary, Research Directions and Current Scope

From the literature review, the authors considered MICP as a reasonable method for stabilizing Sepaku clay shale when biological, chemical, and hydrodynamic parameters are optimized. *Bacillus subtilis* appears to be a potential candidate (especially certain strains) but requires verification of urease/mineralization activity. To properly quantify the effectiveness of MICP for stabilizing Sepaku clay shale, experimental approach should combine: (1) optimization of the MICP protocol (cell density, urea, Ca source, injection method), (2) comprehensive pre/post-treatment characterization (XRD, XRF, SEM/EDS), (3) mechanical testing (UCS, direct shear, slake durability, permeability), and (4) environmental impact analysis (NH_4^+ , pH, conductivity). The authors plan to conduct them in the future.

In this paper, the scope is limited to mechanical testing of slake durability and characterization with XRD and SEM.

3 METHODOLOGY

To optimize MICP stabilization of the Sepaku clay shale, the Sepaku clay shale has to be characterized first. The Sepaku clay shale samples were taken from two soil borings (Figure 11) conducted at Sepaku district (exact location shown in Figure 2). During the soil borings, in addition to disturbed samples, standard penetration tests at 2 m intervals were also conducted. The disturbed samples were used for laboratory tests, namely slaking tests and unconfined compressive strength tests. The slaking tests were conducted using slake durability tool, shown in Figure 12. The tests were conducted in accordance to ASTM D-4644-08 and SNI 3406-2011. While the unconfined compressive strength was tested using a Universal Testing Machine (UTM). Some samples were observed under XRD and also SEM. The XRD was conducted in Universitas Hasanuddin, Mathematics and Natural Sciences Laboratory, while the SEM was conducted at Ujung Pandang Polytechnic Laboratory.



Figure 11. Photographs of soil boring at two locations



Figure 12. Slake durability tool

4 RESULTS AND DISCUSSION

4.1 Boring Log

Figure 12 shows the borelog as well as two enlarged photographs of the core samples. As can be seen from the SPT results, Sepaku clay shale shows rock-like stiffness ($SPT > 60$). The rock-like feature can also be seen from the core box. From the frequency of fractures, it can be seen that the first five meters is less stiff than the final five meters (10 – 15 m). This is to be expected as the clay shale near the ground surface is exposed to weather changes, hence less intact. The borelog description is tabulated in Table 2.

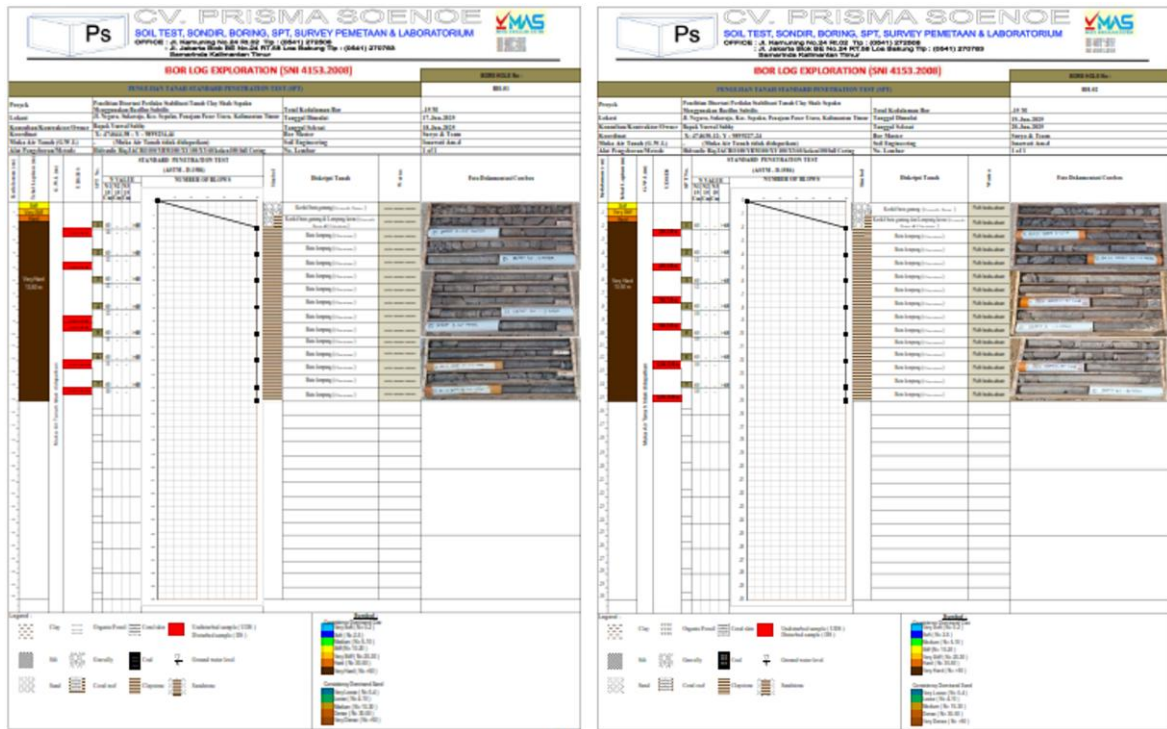


Figure 13. BH. 01 & 02 borelogs, and enlarged photographs of BH-01 coreboxes (0 to 5 m & 10 to 15 m)

Table 2. Borehole data of BH 1 & BH 2 (since both data are identical, the data is only written once)

Depth		Description	N SPT
From	To		
0.0	0.5	Grayish white mountain rock gravel (Stiff)	-
0.5	1.0	Grayish white mountain rock gravel (Very Stiff)	-
1.0	1.5	Grayish white mountain rock gravel & hard clay (Hard)	-
1.5	15	Solid grayish white claystone (Very Hard)	> 60

4.2 Slaking Test

As the clay shale from the two boreholes were similar visually and in terms of N SPT values, the slake durability test was only conducted on samples from depth 2.5 m of BH 1. Figure 14 shows the photographs of the clay shale before the slaking test and after 1, 2 and 3 cycles of slake durability test, while table 3 shows the results.

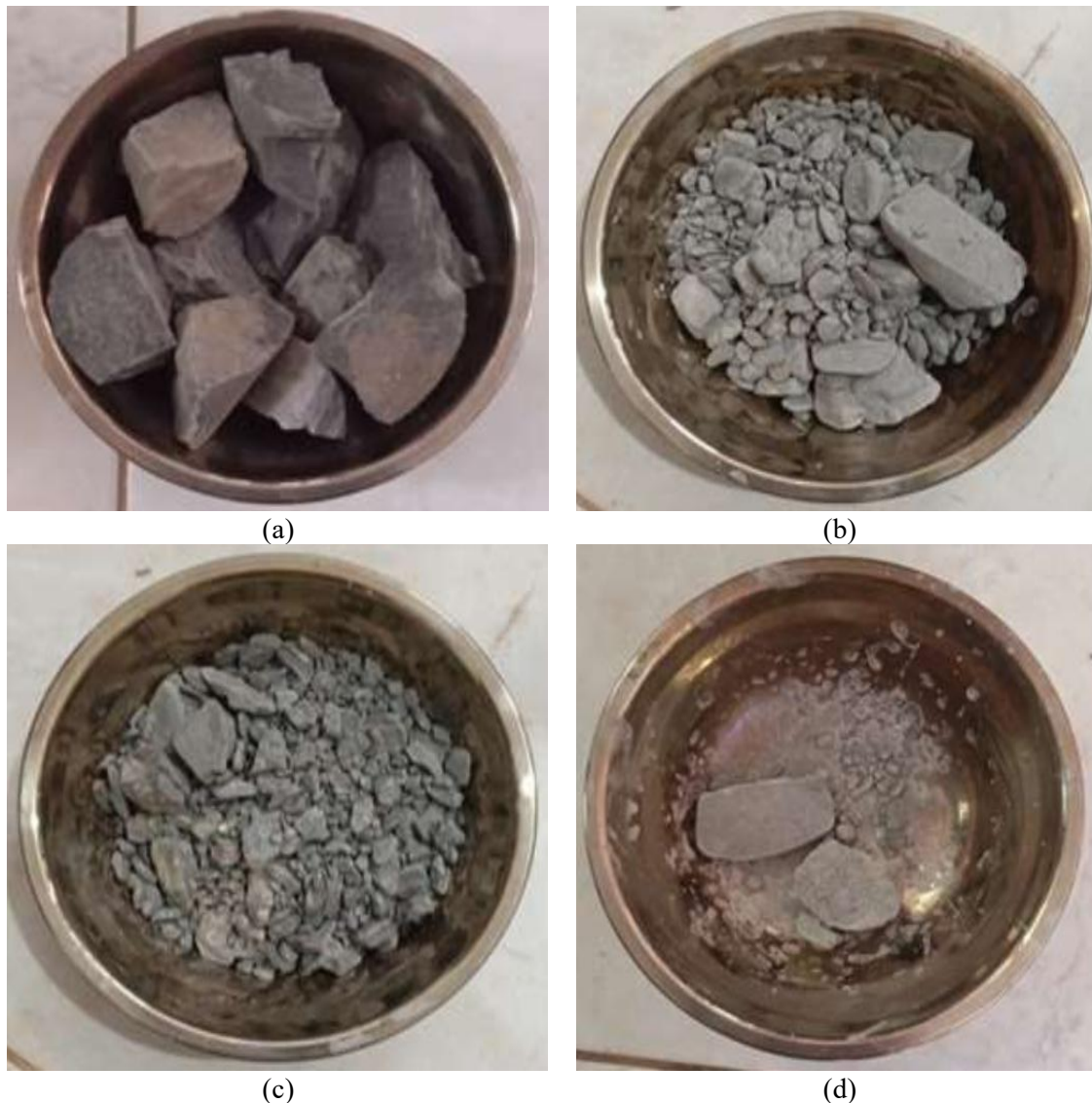


Figure 14. Photograph of the shale: (a) before the test; (b) after cycle 1; (c) after cycle 2; (d) after cycle 3

Table 3. Slake durability test (BH 1)

Description	Clay stone		
Sample weight (grams)	577.9		
Sample dry weight (grams)	509.6		
Moisture content, w (%)	13.40		
Cycle	1	2	3
Sample dry weight after 10 minutes of rotation (grams)	342.1	89.9	39.1
Slake durability index, I_d (%)	67.13	17.64	7.67
Slake durability classification	Very low durability		

The slake durability index (I_d) value is calculated using the following equation:

$$I_d = \frac{W_{final}}{W_{initial}} \times 100\% \quad (3)$$

Where, $W_{initial}$ = initial weight of dry sample (placed in test drum); W_{final} = weight of sample remaining after testing (weighed in dry air).

According to Gamble's (1971) durability classification (Table 4), the Sepaku clay shale is considered low durability after 1 cycle, and very low durability after 2 cycles. Based on the slake durability classification (Table 5), the Sepaku clay shale can be considered very fragile and susceptible to water and wet-dry cycles.

Table 4. Durability classification (Gamble, 1971)

Resilience Class	% Retention after 1 Cycle (10 minutes, Dry Weight)	% Retention after 2 Cycles (10 minutes each)
Very High	> 99	> 98
High	98 – 99	95 – 98
Medium High	95 – 98	85 – 95
Medium	85 – 95	60 – 85
Low	60 – 85	30 – 60
Very Low	< 60	< 30

Table 5. Slake durability classification

Slake durability index (I_d)	Durability classification	Description
< 25%	Very Low Durability	Very fragile, susceptible to water and wet-dry cycles
25 – 50%	Low Durability	Fragile, low resistance to weathering
50 – 75%	Medium Durability	Moderate resistance, partially destroyed when tested
75 – 90%	High Durability	High resistance, only slight damage
> 90%	Very High Durability	Very resistant, almost no damage after testing

4.3 Unconfined Compressive Strength

For the clay shale sample tested under the universal testing machine, the following value was obtained:

Sample diameter, $D = 5.55$ cm, sample height, $h = 14.52$ cm

Maximum load, $P_u = 6.18$ kN, Axial strain on fractures, $\varepsilon = 1\%$

Initial area, $A_0 = \frac{\pi D^2}{4} = 0.002419 \text{ m}^2$

Corrected area (SNI 3683:2012, area correction), $A_c = \frac{A_0}{1-\varepsilon} = \frac{0.002419}{1-0.01} \approx 0.002444 \text{ m}^2$

Unconfined compressive strength, $q_u = \frac{P_u}{A_c} = \frac{6.18}{0.002444} \approx 2529 \text{ kN/m}^2 \approx 2.53 \text{ MPa}$

Undrained shear strength, $s_u \approx \frac{P_u}{2} \approx 1.26 \text{ MPa}$

With a UCS of 2.53 MPa, the Sepaku clay shale is categorized as weak rock based on the Geological Society Engineering Group Working Party (1977).

4.4 XRD and SEM

The XRD test results (Figure 15) are in the form of graphs showing the diffraction patterns of the sample (red) compared to the standard mineral database (blue, pink and green) for mineral identification. The dominant phase appears to be quartz, with strong reflections around $2\theta \approx 26^\circ$ ($d \approx 3.34\text{--}3.40 \text{ \AA}$), indicating a dominant crystalline silica mineral. There is a contribution of clay minerals as a secondary phase, seen from several peaks at low-medium 2θ (e.g., $2\theta \approx 20^\circ \rightarrow d \approx 4.35 \text{ \AA}$, as well as other small peaks) and many small broad peaks typical of argillic/shale samples. Minor phases likely include muscovite/illite or kaolinite and possibly a small amount of feldspar/chlorite, which is hypothetical based on the recorded d-spacing; confirmation requires comparison to a database/treatment diffraction (glycolation/heating).

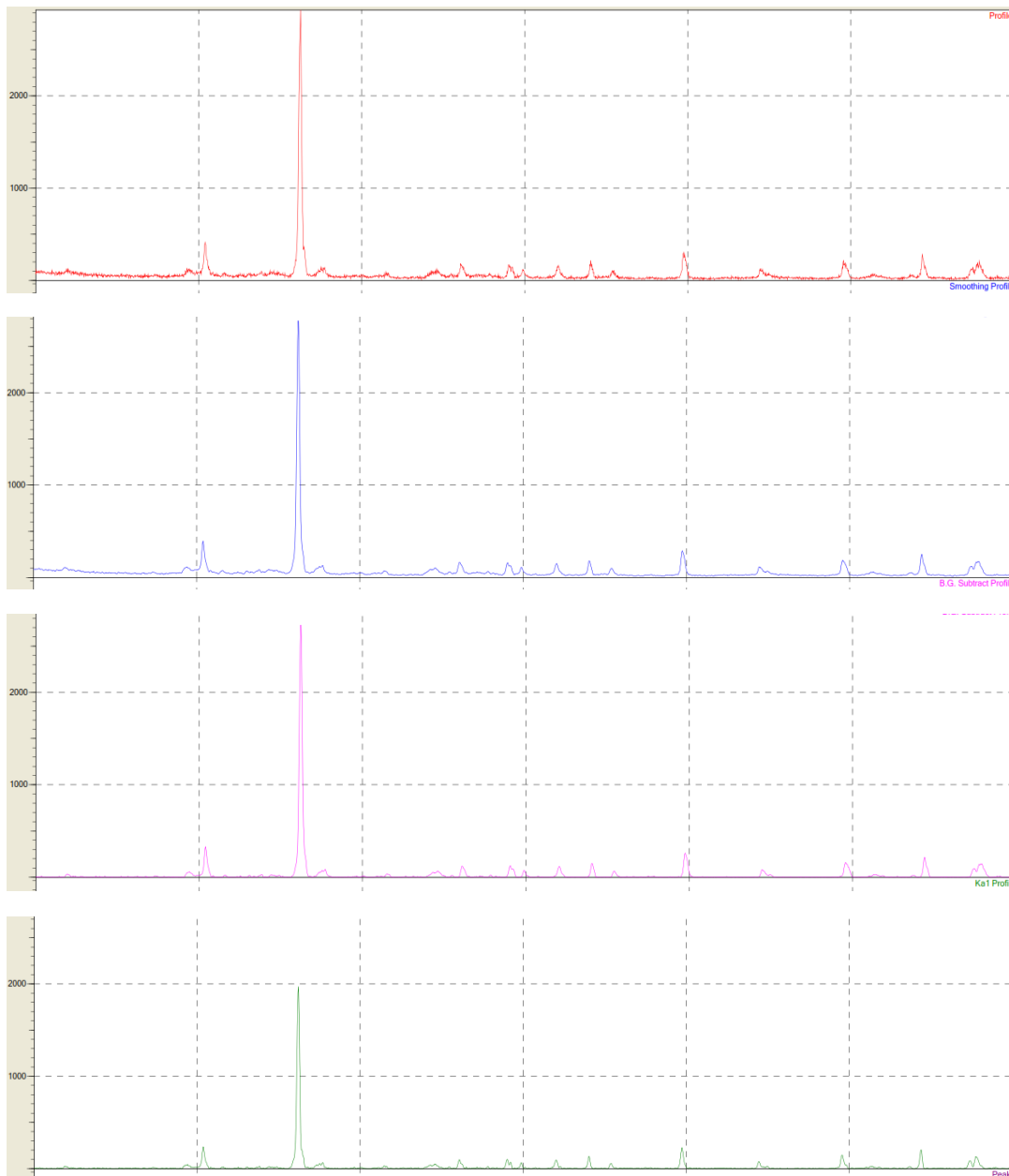


Figure 15. X-Ray diffraction graph of Sepaku clay shale

Figure 16 and 17 show the SEM results of Sepaku clay shale investigated after being crushed, and before being crushed respectively. The SEM magnification used was image interpretation (x5000, WD = 8.4 mm). At this magnification, the lamellar particles can be seen ranging in size from 2–10 μm , stacked together to form dense aggregates. This morphology is characteristic of kaolinite and illite clay minerals, which are generally flat sheets with smooth surfaces that stick together due to Van der Waals forces between particles. In some areas, there are folded and partially rolled sheets, indicating high material plasticity, a property that is also reinforced by XRD results indicating the presence of montmorillonite as a minor expansive mineral. In addition, among these fine layers, several larger particles with a denser shape and slightly rough surface are visible, possibly fine quartz or feldspar grains dispersed in the clay matrix. The presence of these grains agrees with the XRD results, which show strong intensity peaks at 2θ around 26.2° (quartz) and $27\text{--}29^\circ$ (feldspar). In general, the microtexture in this image shows a composite structure between a fine clay matrix and hard silicate grains, which provides a combination of plastic yet sufficiently dense and cohesive mechanical properties. This SEM image thus reinforces the XRD analysis results that the sample is dominated by kaolinite, illite, and quartz minerals, with minor contributions from montmorillonite and feldspar. The layered microstructure pattern indicates a potential for moderate water retention and expansion, typical of clay shale or mudstone materials that have undergone partial diagenesis (Mitchell and Soga, 2005).

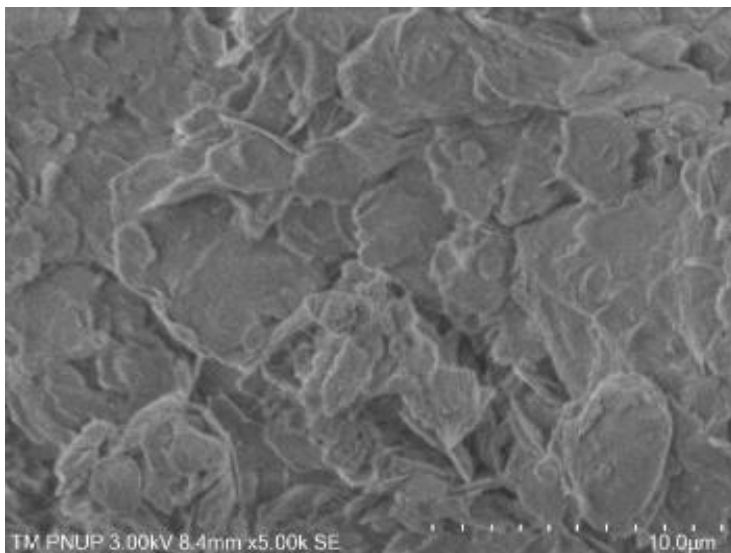


Figure 16. SEM image (powder)

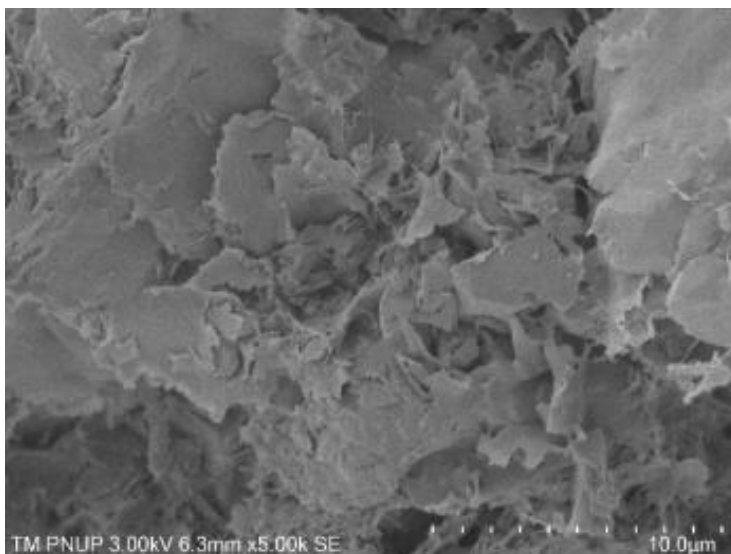


Figure 17. SEM image (stone)

5 CONCLUSIONS

From the samples taken, unweathered Sepaku clay shale shows very hard behavior, with NSPT values above 60. Based on the unconfined compressive strength test, the clay shale can be considered as weak rock. However, upon exposing the clay shale to wetting and drying cycles, and under slaking test conditions, it was found that the Sepaku clay shale has very low durability, with durability index of 17.64% after 2 cycles of wetting and drying.

The XRD shows that the dominant peak (79%) was quartz at 26.6 θ , indicating high silica sand properties, which are very common in quartz sediment materials or residual soil. The secondary peak (10%) was kaolinite at 20.8 θ indicating a clay component (aluminum silicate clay). Minor peaks between 36 θ -50 θ of around 2% indicating the presence of feldspar, illite, chlorite, and mica. The minor peaks show that the material originated from feldspathic weathering or igneous rock. This combination indicates sandy clay soil, with low-medium plasticity and high silica content.

The SEM results of clay shale in rock form, shows a fine, layered clay texture, supporting the XRD results which confirm the presence of kaolinite and illite. The presence of quartz and feldspar indicates the presence of residual minerals from the parent rock. This combination indicates that the material is feldspathic weathered clay, with medium-high plasticity and low permeability.

The data presented in this paper will serve as the basis for future work in stabilizing Sepaku clay through bio-stabilization, namely MICP method.

DISCLAIMER

The authors declare no conflict of interest.

REFERENCES

- Ardebili, P. N., Jozanikohan, G., & Moradzadeh, A., 2025. The Characterization of Clay Minerals in The Kashafrud Formation in a Gas Field in Northeast Iran. *Scientific Reports*, 15, p. 9000. <https://doi.org/10.1038/s41598-025-93930-5>
- Baek, S. H., Kwon, T. H., & DeJong, J. T., 2024. Reductions in hydraulic conductivity of sands caused by microbially induced calcium carbonate precipitation. *Journal of Geotechnical and Geoenvironmental Engineering*, 150(2), 04023134. <https://doi.org/10.1061/JGGEFK.GTENG-11570>
- Bennett, K. C., Berla, L. A., Nix, W. D., & Borja, R. I., 2015. Instrumented nanoindentation and 3D mechanistic modeling of a shale at multiple scales. *Acta Geotechnica*, 10(1), pp. 1-14. <https://doi.org/10.1007/s11440-014-0363-7>
- Bhuiyan, M. H., Agofack, N., Gawel, K. M., & Cerasi, P., 2020. Micro-and macroscale consequences of interactions between CO₂ and shale rocks. *Energies*, 13(5), p. 1167. <https://doi.org/10.3390/en13051167>
- Clarà Saracho, A., Haigh, S. K., Hata, T., Soga, K., Jiang, N. J., & Yamamoto, K., 2025. Experimental Observations of the Effect of MICP on the Deformation Mechanisms of a Layered Formation during Sand Production. *Journal of Geotechnical and Geoenvironmental Engineering*, 151(10), p. 04025107. <https://doi.org/10.1061/JGGEFK.GTENG-12819>
- Chu, J., Stabnikov, V., & Ivanov, V., 2012. Microbially Induced Calcium Carbonate Precipitation on Surface or in the Bulk of Soil. *Geomicrobiology Journal*, 29(6), pp. 544–549. <https://doi.org/10.1080/01490451.2011.592929>
- Etim, R. K., Yohanna, P., Eberemu, A. O., Osinubi, K. J., & Ijimdiya, T. S., 2025. Assessing the biocementation of lateritic soil using hydraulic conductivity and bioinspired optimization approach. *Scientific Reports*, 15(1), p. 27356. <https://doi.org/10.1038/s41598-025-12907-6>

- Fronczyk, J., Marchelina, N., Pyzik, A., & Franus, M., 2023. Assessment of the composition effect of a Bio-cementation Solution on the efficiency of Microbially Induced Calcite precipitation processes in Loose Sandy Soil. *Materials*, 16(17), p. 5767. <https://doi.org/10.3390/ma16175767>
- Fu, T., Saracho, A. C., & Haigh, S. K., 2023. Microbially induced carbonate precipitation (MICP) for soil strengthening: A comprehensive review. *Biogeotechnics*, 1(1), 100002. <https://doi.org/10.1016/j.bgtech.2023.100002>
- Gamble, J. C., 1971. *Durability-plasticity classification of shales and other argillaceous rocks*. Doctoral Thesis, University of Illinois at Urbana-Champaign.
- Geological Society Engineering Group Working Party, 1977. The Description of Rock Masses For Engineering Purposes. Report by the Geological Society Engineering Group Working Party. *Quarterly Journal of Engineering Geology*, 10(4), pp. 355-388.
- Ghasemi, P., & Montoya, B. M., 2022. Field implementation of microbially induced calcium carbonate precipitation for surface erosion reduction of a coastal plain sandy slope. *Journal of Geotechnical and Geoenvironmental Engineering*, 148(9), p. 04022071. [https://doi.org/10.1061/\(ASCE\)GT.1943-5606.0002836](https://doi.org/10.1061/(ASCE)GT.1943-5606.0002836)
- Guo, W., Guo, Y., Cai, Z., Yang, H., Wang, L., Yang, C., Zhao, G., & Bi, Z., 2023. Mechanical behavior and constitutive model of shale under real-time high temperature and high stress conditions. *Journal of Petroleum Exploration and Production Technology*, 13(3), pp. 827-841. <https://doi.org/10.1007/s13202-022-01580-4>
- Gunyol, P., Khosravi, M., Phillips, A., Plymessenger, K., & Parker, A., 2024. Effect of Fines Content on Calcium Carbonate Precipitation and Thermal Properties of Biocemented Sand. *Journal of Geotechnical and Geoenvironmental Engineering (ASCE)*, 150(7), p. 04024047. <https://doi.org/10.1061/JGGEFK.GTENG-11925>
- Han, H., Pang, P., Li, Z., Shi, P., Guo, C., Liu, Y., Chen, S., Lu, J., & Gao, Y. 2019. Controls of organic and inorganic compositions on pore structure of lacustrine shales of Chang 7 member from Triassic Yanchang Formation in the Ordos Basin, China. *Marine and Petroleum Geology*, 100, pp. 270-284. <https://doi.org/10.1016/j.marpetgeo.2018.10.038>
- Harran, R., Terzis, D., & Laloui, L., 2022. Characterizing the deformation evolution with stress and time of biocemented sands. *Journal of Geotechnical and Geoenvironmental Engineering*, 148(10), p. 04022074. [https://doi.org/10.1061/\(ASCE\)GT.1943-5606.0002871](https://doi.org/10.1061/(ASCE)GT.1943-5606.0002871)
- Hoffmann, T. D., Paine, K., & Gebhard, S., 2021. Genetic optimisation of bacteria-induced calcite precipitation in *Bacillus subtilis*. *Microbial cell factories*, 20(1), p. 214. <https://doi.org/10.1186/s12934-021-01704-1>
- Ivanov, V., & Chu, J., 2008. Applications of microorganisms to geotechnical engineering for bioclogging and biocementation of soil in situ. *Reviews in Environmental Science and Bio/Technology*, 7(2), pp. 139-153. <https://doi.org/10.1007/s11157-007-9126-3>
- Ivanov, V., & Stabnikov, V., 2016. Biocementation and biocements. In *Construction biotechnology: biogeochemistry, microbiology and biotechnology of construction materials and processes* (pp. 109-138). Springer Singapore.
- Jia, R., Fu, X., Jin, Y., Wu, T., Wang, S., & Cheng, H., 2023. Mechanical Properties of Mudstone Caprock and Influencing Factors: Implications for Evaluation of Caprock Integrity. *Frontiers in Earth Science*, 11. <https://doi.org/10.3389/feart.2023.1229851>

- Johan, A., Sugianto, A., & Rahardjo, P. P., 2023. Replacement of Weathered Clay Shale Using Soil Cement for Bridge Approach Embankment in Purwakarta – Indonesia. *Indonesian Geotechnical Journal*, 2(3), pp. 123-138. <https://doi.org/10.56144/igj.v2i3.58>
- Lai, H., Ding, X., Cui, M., Zheng, J., Chu, J., & Chen, Z., 2024. Factors affecting the effectiveness of biocementation of soil. *Biogeotechnics*, 2(3), p. 100087. <https://doi.org/10.1016/j.bgtech.2024.100087>
- Lin, H., Dong, Y., Park, J. S., & Montoya, B. M., 2023. Cementation stress characteristic curve for sands treated by microbially induced carbonate precipitation. *Journal of Geotechnical and Geoenvironmental Engineering*, 149(12), 04023115. <https://doi.org/10.1061/JGGEFK.GTENG-11403>
- Liu, B., Tang, C. S., Pan, X. H., Xu, J. J., & Zhang, X. Y., 2024. Suppressing Drought – Induced Soil Desiccation Cracking Using MICP: Field Demonstration and Insights. *Journal of Geotechnical and Geoenvironmental Engineering (ASCE)*, 150(3), p. 04024006. <https://doi.org/10.1061/JGGEFK.GTENG-12011>
- Ma, L., Fauchille, A. L., Ansari, H., Chandler, M., Ashby, P., Taylor, K., Pini, R., & Lee, P. D., 2021. Linking multi-scale 3D microstructure to potential enhanced natural gas recovery and subsurface CO₂ storage for Bowland shale, UK. *Energy & Environmental Science*, 14(8), pp. 4481-4498. <https://doi.org/10.1039/D0EE03651J>
- Mitchell, J. K., & Soga, K., 2005. *Fundamentals of soil behavior*.
- Nazir, R., Rahardjo, P. P., & Mustapha, A. H., 2024. Construction Challenges in Tropical Clay Shale Environments. *Proceedings of International Conference on Geotechnical Engineering Iraq*, pp. 111-120. https://doi.org/10.1007/978-981-97-9364-8_10
- Omoregie, A. I., Wong, C. S., Rajasekar, A., Ling, J. H., Laiche, A. B., Basri, H. F., Sivakumar, G., & Ouahbi, T., 2025. Bio-Based Solutions for Concrete Infrastructure: A Review of Microbial-Induced Carbonate Precipitation in Crack Healing. *Buildings*, 15(7), p. 1052. <https://doi.org/10.3390/buildings15071052>
- Othman, A. G. M., EL-Roudi, A. M., & Tantawy, M. A., 2003. The Physico-ceramic Properties of El-Minia Shale/clay Deposits. *Egyptian Journal of Applied Science*, 18(11B), pp. 469-483.
- Payan, M., Sangdeh, M. K., Salimi, M., Ranjbar, P. Z., Arabani, M., & Hosseinpour, I., 2024. A comprehensive review on the application of microbially induced calcite precipitation (MICP) technique in soil erosion mitigation as a sustainable and environmentally friendly approach. *Results in Engineering*, 24, p. 103235. <https://doi.org/10.1016/j.rineng.2024.103235>
- Qi, Q., Fu, L. Y., Deng, J., & Cao, J., 2021. Attenuation methods for quantifying gas saturation in organic-rich shale and tight gas formations. *Geophysics*, 86(2), D65-D75. <https://doi.org/10.1190/geo2020-0291.1>
- Sagitaningrum, F. H., Kamaruddin, S. A., Soepandji, B. S., & Alatas, M. I., 2023. Review of Clay Shale Soil its Future Research. *Journal of AIP Conference Proceedings*, 2846(1). <https://doi.org/10.1063/5.0154889>
- Said, D., Ibrahim, S. M., Heikal, M., Abdel-Monem, M. O., & Dawwam, G. E., 2025. Bio-mineralization process of CaCO₃ induced by bacteria isolated from Egypt for sustainable bio-concrete. *Microbial Cell Factories*, 24(1), 203. <https://doi.org/10.1186/s12934-025-02837-3>

Shapakidze, E., Avaliani, M., Nadirashvili, M., Maisuradze, V., Gejadze, I., & Petriashvili, T., 2023. Synthesis and Study of Properties of Geopolymer Materials Developed Using Local Natural Raw Materials and Industrial Waste. *Chemistry and Chemical Technology*, 17, pp. 711-718. <https://doi.org/10.23939/chcht17.04.711>

Sidharta, B., & Hasibuan, G., 2022. Mudrock Durability Analysis of Pamaluan Formation in The Region of BWP 1 – IKN (Capital of The Country), Sepaku Region and Surroundings, Penajam Paser Utara Regency, East Kalimantan Province, Indonesia. *Proceedings of PIT IAGI 51st*. <https://www.iagi.or.id/web/digital/71/PITIAGI-22-P-Abs-022.pdf>

Sun, X., Miao, L., Wang, H., Wu, L., Fan, G., & Xia, J., 2022. Sand foreshore slope stability and erosion mitigation based on microbiota and enzyme mix-induced carbonate precipitation. *Journal of Geotechnical and Geoenvironmental Engineering (ASCE)*, 148(8), p. 04022058. [https://doi.org/10.1061/\(ASCE\)GT.1943-5606.0002839](https://doi.org/10.1061/(ASCE)GT.1943-5606.0002839)

Wang, Y. J., Chen, W. B., Yin, J. H., Han, X. L., Zhang, Y., Du, Y. J., & Jiang, N. J., 2024. Role of biochar in drained shear strength enhancement and ammonium removal of biostimulated MICP-treated calcareous sand. *Journal of Geotechnical and Geoenvironmental Engineering (ASCE)*, 150(2), p. 04023140. <https://doi.org/10.1061/JGGEFK.GTENG-11809>

Xiao, Y., Deng, H., Zhu, W., Assefa, E., Cheng, L., Xiong, Y., & Lee, C. F., 2025. Durability Evolution Mechanism of MICP-Treated Calcareous Sand Exposed to Seawater Dry–Wet Cycles. *Journal of Geotechnical and Geoenvironmental Engineering*, 151(8), p. 04025081. <https://doi.org/10.1061/JGGEFK.GTENG-13301>

Zakavi, M., Askari, H., & Shahrooei, M., 2024. Isolation and characterization of a resistance *Bacillus subtilis* for soil stabilization and dust alleviation purposes. *Scientific Reports*, 14(1), p. 25490. <https://doi.org/10.1038/s41598-024-77613-1>

- This page is intentionally left blank -